TCF7L2 plays a complex role in human adipose progenitor biology which may contribute to genetic susceptibility to type 2 diabetes.

Running Title: TCF7L2 and human adipose progenitor biology

Authors: Manu Verma[1], Nellie Y. Loh[1], Senthil K. Vasan[1], Andrea D. van Dam[1], Marijana Todorčević[1], Matt J. Neville[1], Fredrik Karpe[1,2] and Constantinos Christodoulides[1].

Affiliations: [1]Oxford Centre for Diabetes, Endocrinology and Metabolism, Radcliffe Department of Medicine, University of Oxford, Oxford OX3 7LE, UK.

[2]NIHR Oxford Biomedical Research Centre, OUH Foundation Trust, Oxford OX3 7LE, UK.

Address for correspondence to:

Dr Constantinos Christodoulides

Oxford Centre for Diabetes, Endocrinology and Metabolism, Churchill Hospital, Oxford OX3 7LE, UK.

Telephone: +44 (0)1865 857111

E-mail: costas.christodoulides@ocdem.ox.ac.uk

Keywords: Human Adipose Biology, Adipogenesis, Adult Onset Diabetes, WNT Signalling, Human Genetics.

Word count: 3992 words

Number of figures: 6

Number of tables: 0

ABSTRACT

Non-coding genetic variation at *TCF7L2* is the strongest genetic determinant of type 2 diabetes (T2D) risk in humans. TCF7L2 encodes a transcription factor mediating the nuclear effects of WNT signalling in adipose tissue (AT). Here we mapped the expression of *TCF7L2* in human AT and investigated its role in adipose progenitor (AP) biology. APs exhibited the highest *TCF7L2* mRNA abundance compared to mature adipocytes and adipose-derived endothelial cells. Obesity was associated with reduced *TCF7L2* transcript levels in subcutaneous abdominal AT but increased expression in APs. In functional studies, TCF7L2 knockdown (KD) in APs led to dose-dependent activation of WNT/β-catenin signaling, impaired proliferation and dose-dependent effects on adipogenesis. Whilst partial KD enhanced adipocyte differentiation, complete KD impaired lipid accumulation and adipogenic gene expression. Overexpression of TCF7L2 accelerated adipogenesis. Transcriptome-wide profiling revealed that TCF7L2 can modulate multiple aspects of AP biology including extracellular matrix secretion, immune signalling and apoptosis. The T2D-risk allele at rs7903146 was associated with reduced AP *TCF7L2* expression and enhanced AT insulin sensitivity. Our study highlights a complex role for TCF7L2 in AP biology and suggests that in addition to regulating pancreatic insulin secretion, genetic variation at *TCF7L2* may also influence T2D risk by modulating AP function.

INTRODUCTION

Adipose tissue (AT) plays a central role in the regulation of whole-body energy and glucose homoeostasis. Firstly, it provides a safe depot for the storage of excess calories in the form of triglycerides, thereby protecting extra-adipose tissues from lipotoxicity (1). Secondly, it releases energy as free fatty acids during periods of energy demand such as fasting and exercise. Finally, through the secretion of peptide hormones such as leptin and adiponectin it directly regulates systemic energy balance and insulin sensitivity (2). AT expands through an increase in adipocyte number (hyperplasia) and/or size (hypertrophy). Hyperplastic AT growth is mediated *via* generation of new adipocytes from adipose progenitors (APs) and is associated with enhanced systemic insulin sensitivity and an improved glucose and lipid profile. In contrast, adipocyte hypertrophy results in AT inflammation and fibrosis which lead to the development of insulin resistance (3,4).

WNTs are a family of secreted growth factors which function in autocrine and paracrine fashions to regulate stem cell and AP biology (5–7). WNTs signal through frizzled (FZD) receptors to activate multiple downstream signalling cascades. In the best characterized, canonical pathway, WNT binding to FZDs leads to nuclear accumulation of the transcriptional co-activator β-catenin which in conjunction with TCF/LEF transcription factors activates WNT target gene expression. In the absence of WNTs, TCF/LEF proteins are bound to members of the Groucho/TLE family of transcriptional co-repressors and suppress WNT/β-catenin signalling. There are four TCF/LEF family members in mammals; TCF7, TCF7L1, TCF7L2 and LEF1 (8). Of these, TCF7L2 is the most highly expressed in AT (9).

Work from the MacDougald laboratory first highlighted a potential role for TCF7L2 in the regulation of AT function (10). A dominant negative TCF7L2 mutant lacking its β-catenin binding domain was shown to cause spontaneous adipogenesis of 3T3-L1 cells and trans-differentiation of C2C12 myoblasts into adipocytes. More recently, the *in vitro* role of TCF7L2 in the regulation of adipogenesis was revisited with conflicting results. Whilst Chen *et al* showed that TCF7L2 knockdown (KD) in 3T3-L1 preadipocytes leads to impaired adipocyte differentiation (11) in another

study inducible TCF7L2 deletion in immortalised inguinal mouse APs was associated with enhanced adipogenesis (12). *Ex vivo* adipose expression of *Tcf7l2* was suppressed by high-fat diet (HFD)-induced and genetic obesity (12,13). *In vivo*, homozygous global *Tcf7l2* null mice die perinatally whereas heterozygous null animals are lean with enhanced glucose tolerance and insulin sensitivity compared to wild-type controls both on a chow and following a HFD (14). Conversely, transgenic mice over-expressing *Tcf7l2* displayed HFD-induced glucose intolerance (14). Contrasting these findings, targeted deletion of *Tcf7l2* in mature adipocytes (mADs) resulted in enhanced adiposity, glucose intolerance and hyperinsulinaemia (11,12). In humans, *TCF7L2* expression was decreased in the SC abdominal (hereafter referred to as abdominal) AT of subjects with impaired glucose tolerance (11) and reduced systemic insulin sensitivity (15). Notably, non-coding genetic variation at the *TCF7L2* locus was demonstrated to be the strongest genetic determinant of type 2 diabetes (T2D) risk in humans (16,17). The same single nucleotide variation (SNV), rs7903146, was also associated with fat distribution (18). Prompted by these findings we investigated the role of TCF7L2 in human AT function.

RESEARCH DESIGN AND METHODS

Study population: Study subjects were recruited from the Oxford Biobank (www.oxfordbiobank.org.uk), a population-based cohort of healthy 30-50-year-old volunteers (19). Paired abdominal and visceral biopsies were collected from patients undergoing elective surgery as a part of the MolSURG study. Plasma biochemistry (19) and adipocyte sizing (20) were undertaken as described. All studies were approved by the Oxfordshire Clinical Research Ethics Committee, and all volunteers gave written, informed consent.

Cell culture: Primary APs (derived from AT biopsies) or AP lines were cultured and differentiated as described (21,22). Primary endothelial cells were isolated using a CD31 MicroBead Kit (Miltenyi Biotec). Quantification of intracellular lipid was undertaken using AdipoRed lipid stain (Lonza) and multi-well plate reader (PerSeptive Biosystems, Perkin Elmer).

Generation of de-differentiated fat (DFAT) cells: DFAT cells were generated by selection and de-differentiation of lipid-laden, *in vitro* differentiated immortalised APs (23) with modifications (See supplemental information).

Lentiviral constructs and generation of stable AP lines: TCF7L2 (sh843, TRCN0000262843; sh897, TRCN0000061897) and control (scrambled) shRNA plasmid vectors were purchased (Sigma-Aldrich). The TOPflash reporter vector (24) was a gift from Roel Nusse (Addgene #24307). Lentiviral particles were produced in HEK293 cells using MISSION® (Sigma-Aldrich) packaging mix. Stable AP lines were generated by transduction of cells with lentiviral particles and selected using (2µg/ml) puromycin.

Doxycycline-inducible AP lines: The *TCF7L2* sequence (from TCF4E pcDNA3, a kind gift from Frank McCormick, Addgene #32738) (25) was cloned into the tet-pLKO-puro doxycycline-inducible expression lentiviral vector (gift of Dmitri Wiederschain, Addgene #21915) (26). Stable doxycycline-inducible AP lines were generated by transduction of cells with lentiviral particles and selected using (2µg/ml) puromycin.

Proliferation assays: Equal number of APs were seeded, trypsinised and counted using a Cellometer Auto T4 (Nexcelom Bioscience) every 96 hours or using CyQUANT™ cell proliferation assays. Doubling time was calculated using the formula: $T_d = (t_2 - t_1) \times [\log (2) \div \log (q_2 \div q_1)]$, where t = time (days), q = cell number.

Luciferase assays: To asses cis-regulatory activity, a 150 base pair genomic sequence centred around rs7903146 was cloned into a luciferase reporter vector (pGL4.23[luc2/minP], Promega) and co-transfected with pRL-SV40 (Promega) into HEK293 (Lipofectamine 2000) or DFAT cells (Neon Transfection System). 48h post transfection, luciferase activity was assessed using the Dual-Luciferase® Reporter Assay System (Promega) on Veritas Microplate Luminometer (Turner Biosystems).

TOPflash reporter assays: β-catenin transcriptional activity in TCF7L2 KD or overexpressing DFAT cells was determined as described (21).

Real time-PCR and western blots: qRT-PCR and western blotting were performed using TaqMan assays and standard protocols (see supplemental information).

RNA sequencing, pathway enrichment and transcription factor binding-site motif analysis: RNA sequencing (RNA-Seq) was performed in scrambled control, sh897 and sh843 TCF7L2-KD DFAT abdominal APs (see supplemental information). Differentially regulated genes with a false discovery rate <0.05 and an absolute fold-change >1.5, were selected for further analysis. Pathway enrichment and transcription factor binding-site motif analysis were undertaken using Metascape (27) and iRegulon (28), respectively.

Statistical analysis: Statistical analysis was performed using R, SPSS, STATA or GraphPad. For parametric data, Pearson's correlation, two-tailed student's test with Welch's correction (where appropriate) for 2 groups, or one- or two-way ANOVA followed by appropriate *post hoc* tests for multiple groups were used. For non-parametric data, Spearman's correlation, two-tailed Mann-Whitney or Kruskal-Wallis tests were used. Smoothened splines using generalized additive models were used to investigate the relationship between Adipo-IR and BMI in different rs7903146 genotype carriers. p-values were corrected for multiple comparisons or age, BMI and sex (where appropriate) and $p < 0.05$ was considered significant.

RESULTS

TCF7L2 expression is highest in APs. To elucidate the role of TCF7L2 in human AT biology we mapped its expression profile in AT. In biopsy samples from 30 lean and 30 obese individuals, *TCF7L2* mRNA abundance tended to be higher in abdominal *versus* gluteal fat (Fig. 1A). Compared with obese subjects, lean individuals had higher *TCF7L2* expression in abdominal AT. *TCF7L2*

113 transcript levels were similar in the abdominal and visceral AT depots (Fig. 1B). In fractionated AT
114 from over 100 healthy volunteers, *TCF7L2* mRNA levels were higher in APs compared with mADs
115 from both the abdominal and gluteal fat depots (Fig. 1C). Furthermore, in a small sample group (n=5-
116 6), *TCF7L2* expression was higher in APs *versus* adipose-derived endothelial cells (Fig. 1D). Finally,
117 *TCF7L2* mRNA abundance in abdominal APs correlated positively with body mass index (BMI)
118 whilst an opposite trend was detected in abdominal mADs (Fig. 1E, F). No associations between BMI
119 and *TCF7L2* expression in gluteal adipose cell fractions were detected (Fig. S1). Based on these data
120 we focused our subsequent studies on deciphering the function of TCF7L2 in APs.
121
122 ***TCF7L2 dose-dependently modulates AP differentiation.*** We investigated the role of TCF7L2 in
123 AP biology using de-differentiated fat (DFAT) cells generated from immortalised abdominal
124 adipocytes (22). These retain their depot-specific gene expression signature (Fig. S2) and have a
125 higher adipogenic capacity than primary and immortalised APs. Stable KD of TCF7L2 in these cells
126 was achieved with two shRNAs targeting the universal exon 9 of *TCF7L2* (Fig. 2A, B). The first
127 shRNA (sh897) led to 30% KD of TCF7L2 at mRNA level and 68% KD at protein level. The second,
128 more efficient shRNA (sh843), led to 70% reduction in *TCF7L2* expression and near complete
129 TCF7L2 protein KD. KD of TCF7L2 led to impaired AP proliferation (Fig. 2C). No differences in
130 the doubling time of moderate- *versus* high-efficiency TCF7L2-KD cells were detected. Partial
131 TCF7L2-KD was also associated with augmented adipocyte differentiation as ascertained by
132 increased lipid accumulation and enhanced adipogenic gene expression (Fig. 2D - H). In sharp
133 contrast, high-efficiency KD of TCF7L2 resulted in impaired adipogenesis. These findings were
134 confirmed in primary abdominal TCF7L2-KD cells from two subjects. In these latter experiments the
135 anti-adipogenic effect of sh843 was more subtle despite identical TCF7L2-KD efficiency in primary
136 and DFAT cells (Fig. 2I, J). In complimentary experiments we also investigated the effects of
137 inducible *TCF7L2* over-expression on AP functional characteristics using a Tet-On system (Fig. 3).
138 The doxycycline (DOX) dose was selected to induce approximately 2- and 5-fold induction in
139 *TCF7L2* expression compared to vehicle treated *TCF7L2* overexpressing APs which corresponded to
140 an equivalent increase in protein production (and 2.6 and 6.6-fold higher protein production *versus*

vehicle treated empty vector controls) (Fig. 3A, B). AP cells were grown in DOX-free media and *TCF7L2* expression was induced upon plating for proliferation and differentiation experiments and throughout thereafter. Ectopic expression of *TCF7L2* did not influence AP proliferation (Fig. 3C). Low-dose *TCF7L2* overexpression similarly did not affect adipocyte differentiation (Fig. S3) although, the DOX-induced increase in *TCF7L2* expression was not sustained throughout adipogenesis (Fig. S4). On the other hand, 5-fold increase in TCF7L2 protein production accelerated adipocyte differentiation (Fig. S5). By the end of the differentiation time course however, *TCF7L2* over-expressing adipocytes displayed only a subtle increase in lipid accumulation concomitant with increased *CEBPA* expression *versus* vehicle treated controls (Fig. 3D-H). We conclude that, *in vitro* TCF7L2 has dose-dependent actions on adipogenesis.

TCF7L2 dose-dependently modulates WNT/β-catenin signalling. We next determined whether the effects of TCF7L2 on AP function were driven by changes in WNT/β-catenin signalling (Fig. 4). Partial KD of TCF7L2 did not result in altered expression of the universal WNT target gene *AXIN2* (Fig. 4A). In contrast, (near) complete TCF7L2-KD was associated with increased *AXIN2* levels. Using TCF7L2-KD cells stably expressing the TOPflash promoter reporter construct which monitors endogenous β-catenin transcriptional activity we confirmed that complete depletion of TCF7L2 was associated with robust stimulation of canonical WNT signalling whilst weak activation was also seen following partial KD both in the absence and presence of WNT3A (Fig. 4B). Interestingly, despite increased β-catenin transcriptional activity, active β-catenin protein levels were decreased in both sh897 and sh843 cells (Fig. 4C). Given the paradoxical activation of WNT/β-catenin signalling in TCF7L2-KD APs we examined the expression of other TCF/LEF family members in these cells (Fig. 4D & Fig. S6A). Only *TCF7* and *TCF7L1* were expressed in abdominal APs. Notably, TCF7L2-KD was associated with a dose-dependent increase in *TCF7* mRNA abundance in both DFAT and primary abdominal APs (Fig. 4D). In gain-of-function experiments, 48-hour induction of 2- and 5-fold TCF7L2 production did not influence AP *AXIN2* mRNA levels (Fig. 4E). In TOPflash promoter assays, TCF7L2 over-expression led to inhibition of WNT/β-catenin signalling (Fig. 4F, G). However, DOX treatment also suppressed TOPflash activity in empty vector control cells. Over-

169 expression of TCF7L2 did not influence active β-catenin protein levels (Fig. 4I). Collectively these
170 findings suggest that TCF7L2 functions to antagonize the transcriptional activity of β-catenin in
171 abdominal APs.
172
173 ***Transcriptome-wide profiling reveals that TCF7L2 regulates multiple aspects of AP biology.*** To
174 identify the genes and biological processes regulated by TCF7L2 in APs we undertook transcriptomic
175 analyses of TCF7L2-KD cells using RNA-Seq (Fig. 5A). High-efficiency TCF7L2-KD altered the
176 expression of 2,806 genes (18% of all expressed genes) whilst partial KD resulted in a more modest
177 change in the transcriptome with 1,024 genes differentially regulated (FDR < 5%, absolute fold-
178 change > 1.5) (Fig. 5B). Gene set enrichment analysis revealed that the cluster of genes suppressed
179 in complete TCF7L2-KD cells was enriched for pathways and processes involved in cell cycle,
180 response to hypoxia, p53 signalling and ribosome biogenesis (Fig. 5E). Interestingly, cell cycle and
181 ribosome biogenesis are two key pathways that are transcriptionally positively regulated by canonical
182 WNT signalling (29). Consistent with these findings, the expression of many well-established
183 WNT/β-catenin target genes was reduced in high-efficiency TCF7L2-KD APs (Fig. S7). The cluster
184 of upregulated genes in high-efficiency KD cells was enriched for genes involved in interferon
185 signalling and extracellular matrix (ECM) organization. In moderate-efficiency TCF7L2-KD cells
186 the downregulated gene set was also enriched for pathways and processes involved in response to
187 hypoxia and p53 signalling (Fig. 5F). Additionally, we detected enrichment for circadian regulation
188 of gene expression. The upregulated gene cluster in sh897 cells was enriched for genes involved in
189 ECM organization and immune and inflammatory processes. We also performed transcription factor-
190 binding site motif analysis on the promoters of genes differentially expressed in TCF7L2-KD APs
191 (Fig. 5E, F). The promoters of genes suppressed following both complete and partial TCF7L2-KD
192 were enriched for binding sites of E2F4 and FOXM1 which regulate cell proliferation. Genes whose
193 expression was decreased in high-efficiency TCF7L2-KD cells were also enriched for TFDP1,
194 TFDP3 and KLF4 binding sites in their promoters. TFDP family members co-operatively regulate
195 cell cycle genes with members of the E2F family whilst KLF4 suppresses p53 expression and is a β-
196 catenin target gene. The promoters of genes suppressed in partial TCF7L2-KD cells were also

197 enriched for HIF1A binding sites. Genes, whose expression was increased in both sh897 and sh843
198 cells, exhibited enrichment for binding sites of transcription factors involved in cytokine and
199 particularly, interferon signalling in their promoters namely, IRF1, IRF7, STAT1, and STAT2.
200 Finally, real-time PCR revealed good concordance between changes in the transcriptome of DFAT
201 and primary APs following moderate- but not after high-efficiency TCF7L2-KD (Fig. 5G, H).
202
203 ***The T2D-risk allele at rs7903146 reduces AP TCF7L2 expression.*** Genome wide association study
204 (GWAS) meta-analyses have revealed that non-coding genetic variation at *TCF7L2* is the strongest
205 genetic determinant of T2D risk in humans (16,17). Previous efforts to characterize the mechanism
206 of action at *TCF7L2* revealed that the fine-mapped T2D-risk allele at rs7903146 overlaps enhancer
207 histone marks in both islets and APs (30). Whilst this variant has been shown to increase *TCF7L2*
208 expression in islets (31), evidence demonstrating that it is associated with a cis-expression
209 quantitative trait locus (eQTL) in APs has been missing. By examining age-, BMI- and sex-adjusted
210 *TCF7L2* mRNA abundance data in isolated mADs and *ex vivo* cultured abdominal and gluteal APs
211 from up to 21 homozygous carriers of the T2D-risk variant (T) and 59 subjects homozygous for the
212 wild-type allele (C) at rs7903146 we found that the T allele reduces *TCF7L2* expression in abdominal
213 APs (Fig. 6A, B). A similar trend was detected in gluteal APs. We substantiated this finding in a
214 subset of samples by demonstrating lower TCF7L2 protein levels in abdominal APs derived from
215 T2D-risk variant carriers *versus* ancestral allele carriers (Fig. 6C). In cell-based luciferase assays a
216 150 base pair nucleotide genomic sequence centred around rs7903146 exhibited allele-specific
217 enhancer properties in abdominal APs and HEK293 cells with the T allele abolishing enhancer
218 activity (Fig. 6E, F). Histological assessment of abdominal AT biopsies from 19 age- and BMI-
219 matched pairs of males homozygous either for the T2D-risk allele or the protective allele at rs7903146
220 did not reveal any difference in median adipocyte size between the two genotypes (Fig. 6G).
221 However, interrogation of plasma biochemistry data from 600 age- and BMI-matched pairs of
222 subjects from the Oxford Biobank showed that T2D-risk variant carriers had reduced AT insulin
223 resistance (Adipo-IR) (Fig. 6H) which was more pronounced in obese individuals (Fig. 6I). We

conclude that in addition to its established role in regulating pancreatic insulin secretion, genetic variation at rs7903146 may also influence T2D risk through effects on AP biology.

DISCUSSION

Our study highlights a complex role for TCF7L2 in AP biology and AT function. We show that *TCF7L2* expression is similar across different fat depots and diminishes in abdominal AT in obesity. The lower AT *TCF7L2* mRNA abundance in obese subjects could be mediated via increased methylation at *TCF7L2* (32) and may contribute to the AT dysfunction that is associated with greater adiposity. Our results also revealed that *TCF7L2* was highly expressed in all adipose cell lineages examined, namely APs, mature adipocytes and endothelial cells with the former exhibiting the highest transcript levels. These data suggest that TCF7L2 has pleiotropic roles in AT ranging from the regulation of AP biology and adipogenesis, to the modulation of mature adipocyte function and angiogenesis. Finally, we showed that increased adiposity was paradoxically associated with higher *TCF7L2* expression in isolated abdominal APs despite reduced *TCF7L2* mRNA abundance in whole AT. It is likely that the reduction in *TCF7L2* mRNA levels in the abdominal depot in obesity is driven by lower expression in adipocytes given that they are the principal cellular component of AT and as hinted by the correlation data in Fig. 1F. Thus, obesity seems to lead to directionally opposite changes in *TCF7L2* expression in different AT cellular fractions.

To elucidate the role of TCF7L2 in AP biology, we undertook functional studies in immortalised and primary APs. These revealed that TCF7L2 protein production may be regulated both transcriptionally and at the level of protein translation because TCF7L2-KD was associated with more pronounced changes in protein than mRNA levels. Thus in addition to regulating its own transcription (33) TCF7L2 may regulate its own translation. The loss-of-function studies also showed that TCF7L2-KD impairs AP proliferation. Additionally, they demonstrated that TCF7L2 dose-dependently regulates adipogenesis. We speculate that the primary role of TCF7L2 in APs is to restrain adipogenesis since only complete TCF7L2-KD led to impaired adipocyte differentiation whilst

downregulation of its expression within a physiological range, in both DFAT and primary abdominal APs, led to enhanced adipogenesis.

To decipher the signalling pathways mediating the actions of TCF7L2 in AP biology we examined canonical WNT signalling in TCF7L2-KD cells. These experiments revealed that in abdominal APs TCF7L2 may function to inhibit WNT pathway activity. Whilst *prima facie* paradoxical, this result is in keeping with previous findings demonstrating that TCF7L2-KD in 3T3L1 cells was associated with a robust increase in *Axin2* expression (11). Tang *et al* (34) also showed that TCF7L2 displayed a cell-type specific activity to both enhance and inhibit WNT signalling and localized the transcriptional repressive ability of TCF7L2 to its C-terminal tail, which is present in some, so-called E isoforms, but not all *TCF7L2* transcript species. However, expression of E-type *TCF7L2* splice variants is low in AT (35,36). Additionally, none of these studies examined the expression of other TCF/LEF family members in TCF7L2-KD cells (see below). WNT/β-catenin signalling is known to inhibit adipogenesis. Accordingly, high-level KD of TCF7L2 was associated with impaired adipogenesis concomitant with canonical WNT signalling activation. However, downregulation of TCF7L2 expression within a more physiological range (using sh897) led to increased adipocyte differentiation despite mild WNT/β-catenin pathway activation. These data suggest that WNT signalling may have dose-dependent effects on adipogenesis and cell fate determination (21,37). Additionally/alternatively TCF7L2 may engage other signalling pathways to influence AP biology.

To further elucidate the genes, pathways and biological processes regulated by TCF7L2 in APs we undertook genome-wide transcriptional profiling of TCF7L2-KD cells. Consistent with our *in vitro* studies these experiments showed that KD of TCF7L2 activates transcriptional programmes which inhibit the proliferation and modulate the adipogenic capacity of APs. Furthermore, they revealed that TCF7L2 can regulate many aspects of AP biology including ECM secretion, immune and inflammatory signalling, and apoptosis and/or senescence. TCF7L2-KD in APs also led to suppression of HIF1A signalling which promotes fibrosis and AT dysfunction (3). These findings expand the potential functional repertoire of TCF7L2 in AT although, they require experimental

confirmation. Contrary to our expectations, the RNA-Seq experiments also revealed that TCF7L2 promotes canonical WNT signalling in APs. How can we reconcile this finding with our *in vitro* studies? In TCF7L2-KD cells expression of *TCF7* was upregulated. We speculate that TCF7 is a more potent activator of WNT signalling in APs given that functional redundancy is common amongst TCF/LEF family members (8) and based on the increased TOPflash promoter activity and *AXIN2* expression in TCF7L2-KD cells. Nonetheless, increased TCF7 levels cannot compensate for the absence of TCF7L2 at many WNT target gene promoters. Consequently, AP TCF7L2-KD leads to downregulation of several classic WNT target genes and pathways. Transcription factor-binding site analysis was in keeping with the results of the gene set enrichment analysis. Interestingly we saw no enrichment for TCF7L2 binding in the promoters of genes suppressed in TCF7L2-KD cells. However, genome-wide chromatin occupancy data have shown that TCF7L2 regulates gene expression primarily by binding to intergenic regions (29,33). Lastly, the RNA-Seq data provided additional evidence that partial TCF7L2-KD in DFAT cells may be more physiologically relevant as we were better able to replicate changes in the transcriptome of partial *versus* complete TCF7L2-KD DFAT cells in moderate- and high-efficiency TCF7L2-KD primary cells respectively.

GWAS meta-analyses have identified eight independent signals at *TCF7L2* which are associated with T2D susceptibility (17). At least three of these overlap regions of active chromatin in AT (17). Of these signals, only rs7903146 has received attention to date. It has been demonstrated through analysis of GWAS metadata of T2D-related traits (38,39) and human physiological studies (40) that the risk allele at this SNV increases T2D susceptibility *via* impaired insulin secretion. Additionally, this variant was shown to increase *TCF7L2* expression in pancreatic islets (31,41). These data have conclusively established that rs7903146 increases T2D risk primarily through islet dysfunction probably driven by increased *TCF7L2* expression in pancreatic beta-cells. Nevertheless, this SNV may also influence T2D predisposition *via* actions in AT as it was shown to overlap active enhancer histone marks in APs (30) and to be associated with fat distribution (18). Using a “soft clustering” method to group variant-trait associations ascertained from GWAS for 94 independent T2D signals and 47 diabetes-related traits another study also provided some evidence that “lipodystrophy-like”

307 insulin resistance may contribute to T2D predisposition at rs7903146 (39). The same SNV was further
308 shown to overlap a DNA-methylated genomic region exhibiting increased methylation in AT from
309 obese *versus* lean subjects which was reversed post gastric bypass surgery (32). Extending these
310 findings, we now demonstrate that rs7903146 is an eQTL for *TCF7L2* in abdominal APs with the T
311 allele *reducing TCF7L2* expression. Whilst the eQTL signal at rs7903146 was only nominally
312 significant our gene expression data were derived from *ex vivo* expanded APs. This would have added
313 noise to the eQTL dataset in addition to the noise introduced by inter-individual variability in *TCF7L2*
314 AP expression. We also corroborated our data by demonstrating that the T2D-risk variant at this SNV
315 was associated with reduced AP TCF7L2 protein levels and displayed allele specific enhancer activity
316 in luciferase assays which was directional consistent with the eQTL data. Interestingly rs7903146
317 confers higher T2D susceptibility in lean *versus* obese subjects (17). Our results offer a possible
318 explanation for this paradox. In our study the T2D-risk variant at this SNV was associated with
319 enhanced age- and BMI-adjusted AT insulin sensitivity which was more pronounced in obese
320 subjects. Whilst we detected no difference in adipocyte size based on rs7903146 genotype, our study
321 sample (n=19) comprised mostly of lean (n=7) and overweight subjects (n=11) due to limited
322 numbers of obese homozygous T2D-risk allele carriers in the Oxford Biobank (see Fig. 6I). Based
323 on the dose-dependent effects of TCF7L2 on adipogenesis demonstrated herein, it will be interesting
324 to determine whether the T2D-predisposing allele at rs7903146 is associated with differential effects
325 on adipocyte size in lean *versus* obese subjects; with smaller fat cells specifically seen in obese
326 individuals which have higher baseline AP *TCF7L2* expression.
327
328 In summary, our work highlights that TCF7L2 plays an important but complex role in AP biology.
329 We also demonstrate that rs7903146 has *cis* regulatory effects outside the pancreas and reduces
330 *TCF7L2* expression in abdominal APs. Thus, in addition to islet dysfunction, altered AP function
331 consequent to changes in *TCF7L2* expression might also influence the T2D predisposition conferred
332 by this SNV. Future studies should define the role of TCF7L2 in human adipocytes and characterize
333 the impact of T2D-associated regulatory variants at *TCF7L2*, beyond rs7903146, which overlap open
334 chromatin in adipose cells on adipose *TCF7L2* expression and AT function.

ACKNOWLEDGEMENTS

We thank the volunteers from the Oxford BioBank (www.oxfordbiobank.org.uk) for their participation in this recall study. We thank the nurses at the Clinical Research Unit, in particular, Mrs. Jane Cheeseman, for their help in recruitment and sample collection from Oxford BioBank volunteers. The OBB and Oxford BioResource are funded by the NIHR Oxford Biomedical Research Centre (BRC). The views expressed are those of the author(s) and not necessarily those of the NIHR or the Department of Health and Social care. This research is supported by the British Heart Foundation through an Intermediate Clinical Research Fellowship to CC (FS/16/45/32359) and a programme grant (RG/17/1/32663) to FK. MV and ADVD are supported by a Novo Nordisk Postdoctoral Fellowship run in partnership with the University of Oxford. Funding support was also received from the National Institute for Health Research, Oxford Biomedical Research Centre (BRC). We thank the Oxford Genomics Centre at the Wellcome Centre for Human Genetics (funded by Wellcome Trust grant reference 203141/Z/16/Z) for the generation of the Sequencing data. The Genotype-Tissue Expression (GTEx) Project was supported by the Common Fund of the Office of the Director of the National Institutes of Health, and by NCI, NHGRI, NHLBI, NIDA, NIMH, and NINDS. The data used for the analyses described in this manuscript were obtained from the GTEx Portal on 10/20/19.

CONTRIBUTION STATEMENT

Conceptualization, C.C.; Methodology, M.V., N.Y.L., S.K.V.; Investigation, M.V., N.Y.L., S.K.V., A.D.V.D., M.T., M.J.N., C.C., Writing – Original Draft, M.V., C.C.; Writing – Review & Editing, All authors; Funding Acquisition, C.C., F.K., Resources, C.C., F.K.; Supervision, C.C., F.K. C.C is the guarantor of this work and, as such, had full access to all the data in the study and takes responsibility for the integrity of the data and the accuracy of the data analysis.

DUALITY OF INTEREST

MV and ADVD are supported by a Novo Nordisk Postdoctoral Fellowship run in partnership with the University of Oxford. The funders had no role in study design, analysis or reporting of the current work. The authors declare that there is no duality of interest associated with this manuscript.

PRIOR PRESENTATIONS: Parts of the study were presented as an oral presentation at the 54th Annual Meeting of European Association for the Study of Diabetes, Berlin, Germany, 1-5th October 2018 and at the 44th Adipose Tissue Discussion Group meeting, Edinburgh, UK, 6-7th December 2018.

REFERENCES

1. Mann JP, Savage DB. What lipodystrophies teach us about the metabolic syndrome. J Clin Invest. 2019;129(10):4009–21.
2. Kahn CR, Wang G, Lee KY. Altered adipose tissue and adipocyte function in the pathogenesis of metabolic syndrome. J Clin Invest. 2019;129(10):3990–4000.
3. Sun K, Tordjman J, Clément K, Scherer PE. Fibrosis and adipose tissue dysfunction. Cell Metab. 2013;18(4):470–7.
4. Marcelin G, Silveira ALM, Martins LB, Ferreira AVM, Clément K. Deciphering the cellular interplays underlying obesity-induced adipose tissue fibrosis. J Clin Invest. 2019;129(10):4032–40.
5. Prestwich TC, MacDougald OA. Wnt/β-catenin signaling in adipogenesis and metabolism. Curr Opin Cell Biol. 2007;19(6):612–7.
6. Christodoulides C, Lagathu C, Sethi JK, Vidal-Puig A. Adipogenesis and WNT signalling. Trends Endocrinol Metab. 2009;20(1):16–24.
7. Nusse R, Clevers H. Wnt/β-Catenin Signaling, Disease, and Emerging Therapeutic Modalities. Cell [Internet]. 2017;169(6):985–99. Available from: http://dx.doi.org/10.1016/j.cell.2017.05.016
8. Cadigan KM, Waterman ML. TCF/LEFs and Wnt signaling in the nucleus. Cold Spring Harb Perspect Biol. 2012;4(11):1–22.
9. Aguet F, Brown AA, Castel SE, Davis JR, He Y, Jo B, et al. Genetic effects on gene expression across human tissues. Nature. 2017;550(7675):204–13.
10. Ross SE, Hemati N, Longo KA, Bennett CN, Lucas PC, Erickson RL, et al. Inhibition of Adipogenesis by Wnt Signaling. Science (80-). 2000;289(5481).
11. Chen X, Ayala I, Shannon C, Fourcaudot M, Acharya NK, Jenkinson CP, et al. The diabetes gene and wnt pathway effector TCF7L2 regulates adipocyte development and function. Diabetes. 2018;67(4):554–68.
12. Geoghegan G, Simcox J, Seldin MM, Parnell TJ, Stubben C, Just S, et al. Targeted deletion of Tcf7l2 in adipocytes promotes adipocyte hypertrophy and impaired glucose metabolism. Mol Metab [Internet]. 2019;24(March):44–63. Available from: https://doi.org/10.1016/j.molmet.2019.03.003
13. Chen ZL, Shao WJ, Xu F, Liu L, Lin BS, Wei XH, et al. Acute Wnt pathway activation positively regulates leptin gene expression in mature adipocytes. Cell Signal [Internet]. 2015;27(3):587–97. Available from: http://dx.doi.org/10.1016/j.cellsig.2014.12.012
14. Yang H, Li Q, Lee JH, Shu Y. Reduction in Tcf7l2 expression decreases diabetic susceptibility in mice. Int J Biol Sci. 2012;8(6):791–801.
15. Karczewska-Kupczewska M, Stefanowicz M, Matulewicz N, Nikołajuk A, Straczkowski M.

Wnt signaling genes in adipose tissue and skeletal muscle of humans with different degrees of insulin sensitivity. J Clin Endocrinol Metab. 2016;101(8):3079–87.

16. Cauchi S, El Achhab Y, Choquet H, Dina C, Krempler F, Weitgasser R, et al. TCF7L2 is reproducibly associated with type 2 diabetes in various ethnic groups: a global meta-analysis. J Mol Med [Internet]. 2007 Jul 3 [cited 2016 Nov 17];85(7):777–82. Available from: http://link.springer.com/10.1007/s00109-007-0203-4
17. Mahajan A, Taliun D, Thurner M, Robertson NR, Torres JM, Rayner NW, et al. Fine-mapping type 2 diabetes loci to single-variant resolution using high-density imputation and islet-specific epigenome maps. Nat Genet. 2018;50(11):1505–13.
18. Pulit SL, Stoneman C, Morris AP, Wood AR, Glastonbury CA, Tyrrell J, et al. Meta-Analysis of genome-wide association studies for body fat distribution in 694 649 individuals of European ancestry. Hum Mol Genet. 2019;28(1):166–74.
19. Karpe F, Vasan SK, Humphreys SM, Miller J, Cheeseman J, Dennis AL, et al. Cohort profile: The Oxford Biobank. Int J Epidemiol. 2018;47(1):21-21g.
20. Small KS, Todorčević M, Civelek M, El-Sayed Moustafa JS, Wang X, Simon MM, et al. Regulatory variants at KLF14 influence type 2 diabetes risk via a female-specific effect on adipocyte size and body composition. Nat Genet. 2018;50(4):572–80.
21. Loh NY, Neville MJ, Marinou K, Hardcastle SA, Fielding BA, Duncan EL, et al. LRP5 regulates human body fat distribution by modulating adipose progenitor biology in a dose- and depot-specific fashion. Cell Metab [Internet]. 2015 Feb 3 [cited 2016 Oct 10];21(2):262–72. Available from: http://dx.doi.org/10.1016/j.cmet.2015.01.009
22. Todorčević M, Hilton C, McNeil C, Christodoulides C, Hodson L, Karpe F, et al. A cellular model for the investigation of depot specific human adipocyte biology. Adipocyte [Internet]. 2017;6(1):40–55. Available from: https://www.tandfonline.com/doi/full/10.1080/21623945.2016.1277052
23. Lessard J, Côté JA, Lapointe M, Pelletier M, Nadeau M, Marceau S, et al. Generation of human adipose stem cells through dedifferentiation of mature adipocytes in ceiling cultures. J Vis Exp. 2015;2015(97):1–5.
24. Fuerer C, Nusse R. Lentiviral vectors to probe and manipulate the Wnt signaling pathway. PLoS One. 2010;5(2).
25. Tetsu O, McCormick F. β-catenin regulates expression of cyclin D1 in colon carcinoma cells. Nature. 1999;398(6726):422–6.
26. Wiederschain D, Wee S, Chen L, Loo A, Yang G, Huang A, et al. Single-vector inducible lentiviral RNAi system for oncology target validation. Cell Cycle. 2009;8(3):498–504.
27. Zhou Y, Zhou B, Pache L, Chang M, Khodabakhshi AH, Tanaseichuk O, et al. Metascape provides a biologist-oriented resource for the analysis of systems-level datasets. Nat Commun [Internet]. 2019;10(1). Available from: http://dx.doi.org/10.1038/s41467-019-09234-6
28. Janky R, Verfaillie A, Imrichová H, van de Sande B, Standaert L, Christiaens V, et al. iRegulon: From a Gene List to a Gene Regulatory Network Using Large Motif and Track Collections. PLoS Comput Biol. 2014;10(7).
29. Madan B, HARMSTON N, Nallan G, Montoya A, Faull P, Petretto E, et al. Temporal dynamics of Wnt-dependent transcriptome reveals an oncogenic Wnt / MYC / ribosome axis Graphical abstract Find the latest version : J Clin Invest [Internet]. 2018;128(12):5620–33. Available from: http://www.jci.org/articles/view/122383
30. Varshney A, Scott LJ, Welch RP, Erdos MR, Chines PS, Narisu N, et al. Genetic regulatory signatures underlying islet gene expression and type 2 diabetes. Proc Natl Acad Sci U S A. 2017;114(9):2301–6.
31. Lyssenko V, Lupi R, Marchetti P, Del Guerra S, Orho-Melander M, Almgren P, et al. Mechanisms by which common variants in the TCF7L2 gene increase risk of type 2 diabetes. JClinInvest. 2007;117(8):2155–63.
32. Multhaup ML, Seldin MM, Jaffe AE, Lei X, Kirchner H, Mondal P, et al. Mouse-human experimental epigenetic analysis unmasks dietary targets and genetic liability for diabetic phenotypes. Cell Metab. 2015;21(1):138–49.
33. Hatzis P, van der Flier LG, van Driel MA, Guryev V, Nielsen F, Denissov S, et al. Genome-Wide Pattern of TCF7L2/TCF4 Chromatin Occupancy in Colorectal Cancer Cells. Mol Cell

462 Biol. 2008;28(8):2732–44.
463 34. Tang W, Dodge M, Gundapaneni D, Michnoff C, Roth M, Lum L. A genome-wide RNAi
464 screen for Wnt/beta-catenin pathway components identifies unexpected roles for TCF
465 transcription factors in cancer. Proc Natl Acad Sci U S A [Internet]. 2008;105(28):9697–702.
466 Available from:
467 http://www.pubmedcentral.nih.gov/articlerender.fcgi?artid=2453074&tool=pmcentrez&rend
468 ertype=abstract
469 35. Kaminska D, Kuulasmaa T, Venesmaa S, Käkelä P, Vaittinen M, Pulkkinen L, et al. Adipose
470 tissue TCF7L2 Splicing is regulated by weight loss and associates with glucose and fatty acid
471 metabolism. Diabetes. 2012;61(11):2807–13.
472 36. Mondal AK, Das SK, Baldini G, Chu WS, Sharma NK, Hackney OG, et al. Genotype and
473 tissue-specific effects on alternative splicing of the transcription factor 7-like 2 gene in
474 humans. J Clin Endocrinol Metab. 2010;95(3):1450–7.
475 37. Basham KJ, Rodriguez S, Turcu AF, Lerario AM, Logan CY, Rysztak MR, et al. A ZNRF3-
476 dependent Wnt/β-catenin signaling gradient is required for adrenal homeostasis. Genes Dev.
477 2019;33(3–4):209–20.
478 38. Mahajan A, Wessel J, Willems SM, Zhao W, Robertson NR, Chu AY, et al. Refining the
479 accuracy of validated target identification through coding variant fine-mapping in type 2
480 diabetes article. Nat Genet. 2018;50(4):559–71.
481 39. Udler MS, Kim J, von Grotthuss M, Bonàs-Guarch S, Cole JB, Chiou J, et al. Type 2 diabetes
482 genetic loci informed by multi-trait associations point to disease mechanisms and subtypes: A
483 soft clustering analysis. PLoS Med. 2018;15(9):1–23.
484 40. Ingelsson E, Langenberg C, Hivert MF, Prokopenko I, Lyssenko V, Dupuis J, et al. Detailed
485 physiologic characterization reveals diverse mechanisms for novel genetic loci regulating
486 glucose and insulin metabolism in humans. Diabetes. 2010;59(5):1266–75.
487 41. Viñuela A, Varshney A, Bunt M van de, Prasad RB, Asplund O, Bennett A, et al. Influence of
488 genetic variants on gene expression in human pancreatic islets – implications for type 2
489 diabetes. bioRxiv [Internet]. 2019;(d):655670. Available from:
490 https://www.biorxiv.org/content/10.1101/655670v1
491

492 **FIGURE LEGENDS**

493 **Fig. 1 *Ex vivo TCF7L2* expression in human adipose depots and adipose cell fractions.** *TCF7L2*
494 expression in paired samples of (A) subcutaneous abdominal and gluteal adipose tissue (AT) biopsies
495 from lean and obese subjects (n=30 [15F] / group; Lean – Age 43.9±4.7 years, BMI 22.0±1.1 kg/m^2;
496 Obese – Age 43.9±3.6 years, BMI 34.5±2.4 kg/m^2), (B) abdominal subcutaneous and visceral AT
497 biopsies (n=27 [16F] / group; Age - 59.1±11.8 years, BMI - 28.2±7.2 kg/m^2), (C) cultured APs and
498 mature adipocytes (mADs) from subcutaneous abdominal and gluteal AT biopsies (n=108-114 [59F]
499 / group; Age - 45.3±8.7 years, BMI - 27.2±4.5 kg/m^2), and (D) cultured APs and adipose-derived
500 endothelial cells from subcutaneous abdominal and gluteal AT biopsies (n=5-6 [5-6F] / group; Age -
501 51.9±7.9 years, BMI - 28.8±4.0 kg/m^2). Errror bars are mean ± SD. (E, F) Correlations between
502 *TCF7L2* expression in cultured APs and mADs from subcutaneous abdominal AT biopsies and donor
503 BMI (n=110-113 [59F] / group; Age - 45.3±8.7 years, BMI - 27.2±4.5 kg/m^2). qRT-PCR data were

normalized to geometric mean of (A) *PPIA*, *PGK1*, *PSMB6*, and *IPO8*, (B) *PPIA* and *PGK1*, or (C-F) to 18S rRNA levels. ***p<0.001; $^{\#}$p<0.05 (adjusted for multiple comparisons). Histograms are means ± SEM. Age and BMI data are means ± SD.

Fig. 2 TCF7L2 KD in abdominal APs impairs proliferation and dose-dependently regulates differentiation. (A-H) TCF7L2 KD in DFAT abdominal APs. shCN = scrambled control, sh897 = moderate and sh843 = high TCF7L2 KD DFAT abdominal APs. TCF7L2 KD was confirmed by (A) qRT-PCR and (B) western blot in DFAT abdominal APs. (C) Doubling time of control, sh897 and sh843 TCF7L2 KD APs. (D) Representative micrographs of control, sh897 and sh843 APs at day 14 of adipogenic differentiation. The histogram shows the relative lipid accumulation (as a marker for differentiation) assessed by AdipoRed lipid stain (n=24 wells/group), (E-H) Relative mRNA levels of adipogenic genes *CEBPA*, *PPARG2*, *FABP4* and *ADIPOQ* at baseline (day 0), day 7 and day 14 of adipogenic differentiation. **(I-J)** TCF7L2 KD in human primary abdominal APs. (I) Confirmation of TCF7L2 KD by qRT-PCR and western blot in human primary abdominal APs (western blots from one experiment). (J) Representative micrographs of control, moderate (sh897) and high (sh843) TCF7L2 KD human primary abdominal APs at day 14 of adipogenic differentiation. The histogram shows the relative lipid accumulation, assessed by AdipoRed (n=16 wells/group). qRT-PCR data were normalized to 18S rRNA levels. Histograms are means ± SEM. Data obtained from 3 independent experiments. ***p<0.001, **p<0.01; $^{\#\#\#}$p<0.001, $^{\#\#}$p<0.01, $^{\#}$p<0.05 (adjusted for multiple comparisons). α-tubulin was used as a loading control for western blots.

Fig. 3 Doxycycline-induced TCF7L2 overexpression in DFAT abdominal APs regulates adipogenesis. DFAT abdominal APs, stably transduced with the empty vector (EV) or TCF7L2 overexpression vector (TCF7L2), were cultured in the presence of vehicle (Veh) or DOX (final concentration: 0.01 μg/ml or 0.05 μg/ml) to induce TCF7L2 overexpression. TCF7L2 overexpression was confirmed by (A) qRT-PCR and (B) western blot in DFAT abdominal APs. (C) Doubling time of DFAT abdominal APs. (D) Representative micrographs of DFAT abdominal APs at day 14 of adipogenic differentiation. The histogram shows the relative lipid accumulation, assessed by

AdipoRed lipid stain (n=24 wells/group). (E-H) Relative mRNA levels of adipogenic genes *CEBPA*, *PPARG2*, *FABP4* and *ADIPOQ* at day 14 of adipogenic differentiation. qRT-PCR data were normalized to 18S rRNA levels. Histograms are means ± SEM and expressed relative to vehicle-treated cells (arbitrarily set to 1). Data obtained from 3 independent experiments. ***p<0.001, **p<0.01, *p<0.05; $^{###}$p<0.001, $^{#}$p<0.05 (adjusted for multiple comparisons). Actin was used as western blot loading control.

Fig. 4 TCF7L2 dose-dependently modulates WNT/β-catenin signalling. (A-D) Effects of TCF7L2 KD on: (A) *AXIN2* mRNA levels, (B) TOPFlash promoter activity following 6h treatment with vehicle (Veh) or 50ng/ml WNT3A (n=12 wells/group), (C) active β-catenin protein levels, and (D) *TCF7* mRNA levels. shCN = scrambled control, sh897 = moderate and sh843 = high TCF7L2 KD DFAT abdominal APs. **(E-I)** Effects of TCF7L2 overexpression on: (E) *AXIN2* mRNA levels, (F and G) TOPFlash promoter activity following 20h treatment with (F) vehicle (Veh) or (G) 50ng/ml WNT3A (n=12 wells/group), (H) *TCF7* mRNA levels, and (I) active β-catenin protein levels. DFAT abdominal APs expressing either the empty vector (EV) or TCF7L2 overexpression vector (TCF7L2) were cultured in the presence of vehicle (Veh) or DOX (final concentration of 0.01 µg/ml or 0.05 µg/ml). Data expressed relative to vehicle treatment (arbitrarily set to 1) for EV or TCF7L2 overexpressing DFAT abdominal AP line, respectively. Actin was used as a loading control for western blots. qRT-PCR data were normalized to 18S rRNA levels. Histograms are means ± SEM. Data obtained from 3 independent experiments. ***p<0.001, **p<0.01, *p<0.05; $^{###}$p<0.001, $^{##}$p<0.01, $^{#}$p<0.05 (adjusted for multiple comparisons).

Fig. 5 Global transcriptional profiling reveals that TCF7L2 regulates multiple aspects of AP biology. (A) Principal component analysis (PCA) of the global transcriptomic profile of control (scrambled), moderate (sh897) and high (sh843) TCF7L2 KD DFAT abdominal APs. (B) Venn diagram showing the overlap between differentially regulated genes from paired comparisons (FDR<0.05; absolute fold change >1.5). (C and D) Volcano plots showing the genes differentially regulated between control and (C) sh897; or (D) sh843, TCF7L2 KD DFAT abdominal APs.

Highlighted are the top 20 differentially regulated genes. (E and F) Pathway enrichment analyses of genes downregulated (red) and upregulated (green) in (E) sh897 and (F) sh843 DFAT abdominal APs, *vs.* controls. Shown also are transcription factor binding-site motif analysis (inset) of downregulated (red) and upregulated (green) genes. (G and H) qRT-PCR validation of differentially regulated genes. qRT-PCR data were normalized to 18S rRNA levels and are from 3 independent experiments. Histograms are means ± SEM. FDR is annotated for RNA-Seq fold-change measurements. ***p<0.001, **p<0.01, *p<0.05 for qRT-PCR measurements.

Fig. 6 The type 2 diabetes risk allele at rs7903146 reduces TCF7L2 expression in human abdominal APs. (A and B) *TCF7L2* expression in paired cultured APs and mature adipocytes (mADs) from subcutaneous (A) abdominal and (B) gluteal AT biopsies from homozygous carriers of the T2D allele T (n=19-21 [4F]) *vs.* carriers of the non-risk allele C (n=54-59 [29F]). TT carriers, Age - 42.8±6.4 years, BMI - 26.2±6.0 kg/m^2. CC carriers, Age - 45.8±9.5 years, BMI - 27.3±3.8 kg/m^2. p-value adjusted for age, BMI and sex. (C) TCF7L2 protein levels in cultured abdominal APs from age-, BMI- and sex-matched homozygous carriers of the T2D risk allele T *vs.* carriers of the non-risk allele C (n=11/group). Actin was used as western blot loading control. (D) Chromatin state map showing that rs7903146 overlaps a weak enhancer in APs (image reproduced from type2diabetesgenetics.org). Yellow – weak enhancer, orange – active enhancer, green – transcription (E and F) Luciferase reporter assay in (E) DFAT abdominal APs and (F) HEK293 cells transfected with empty vector (EV) or the luciferase reporter vector containing 151 bp genomic sequence with the T2D risk allele T or the non-risk allele C (n=12-16 replicates/group). ***p<0.001; $^{\#\#\#}$p<0.001, $^{\#}$p<0.05 (adjusted for multiple comparisons). (G) Median adipocyte area (µm^2) calculated from the histological sections of abdominal AT from 19 pairs of age- and BMI-matched males grouped by rs7903146 genotype. CC carriers, Age - 44.2±6.3 years, BMI - 25.4±2.8 kg/m^2. TT carriers, Age - 44.1±7.3 years, BMI - 25.1±2.7 kg/m^2. Error bars are median with 95% CI. (H) Comparison of adipose tissue insulin resistance (Adipo-IR) between age-, BMI- and sex-matched homozygous carriers of the T2D risk allele (T) and the non-risk allele (C) (n= 600 pairs). **p<0.01. Data are medians with boxplot showing IQR and whiskers are range of values within 1.5*IQR. (I) Smoothened

588 splines showing the relationship between adipo-IR and BMI for homozygous carriers of the T2D risk
589 allele (T) and carriers of the non-risk allele (C) at rs7903146. See Table S1 for anthropometric and
590 plasma biochemistry data for (H and I).

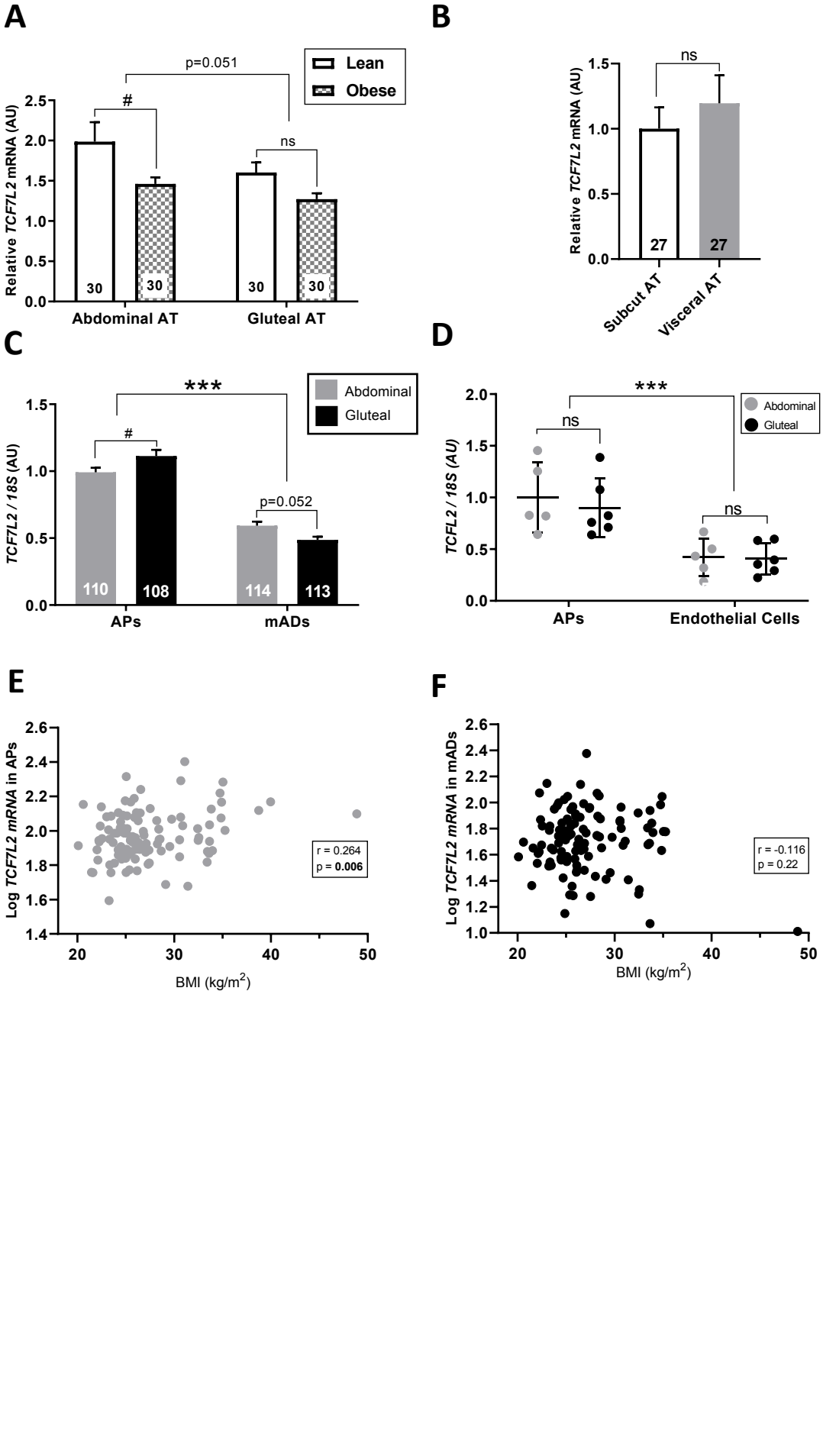
A
p=0.051
Lean
Obese
#
ns
Relative TCF7L2 mRNA (AU)
2.5
2.0
1.5
1.0
0.5
0.0
30
30
30
30
Abdominal AT
Gluteal AT
B
ns
Relative TCF7L2 mRNA (AU)
1.5
1.0
0.5
0.0
27
27
Subcut AT
Visceral AT
C
***
Abdominal
Gluteal
#
p=0.052
TCF7L2 / 18S (AU)
1.5
1.0
0.5
0.0
110
108
114
113
APs
mADs
D
***
ns
ns
Abdominal
Gluteal
TCFL2 / 18S (AU)
2.0
1.5
1.0
0.5
0.0
APs
Endothelial Cells
E
Log TCF7L2 mRNA in APs
2.6
2.4
2.2
2.0
1.8
1.6
1.4
r = 0.264
p = 0.006
20
30
40
50
BMI (kg/m2)
F
Log TCF7L2 mRNA in mADs
2.6
2.4
2.2
2.0
1.8
1.6
1.4
1.2
1.0
r = -0.116
p = 0.22
20
30
40
50
BMI (kg/m2)

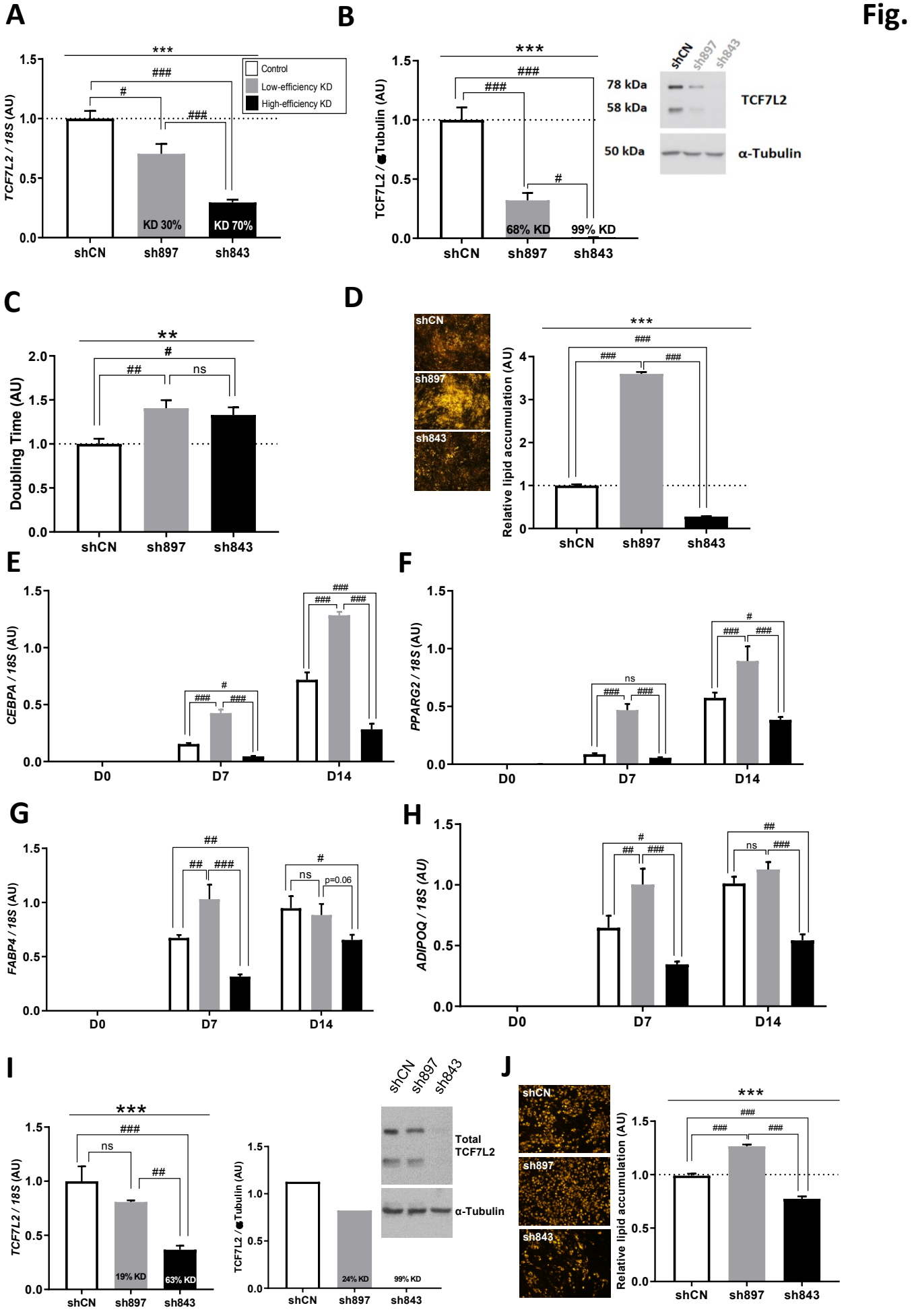
A
B
C
D
E
F
G
H
I
J
Control
Low-efficiency KD
High-efficiency KD
TCF7L2 / 18S (AU)
KD 30%
KD 70%
shCN
sh897
sh843
TCF7L2 / αTubulin (AU)
78 kDa
58 kDa
50 kDa
TCF7L2
α-Tubulin
68% KD
99% KD
Doubling Time (AU)
ns
Relative lipid accumulation (AU)
CEBPA / 18S (AU)
PPARG2 / 18S (AU)
FABP4 / 18S (AU)
ADIPOQ / 18S (AU)
D0
D7
D14
p=0.06
19% KD
63% KD
24% KD
Total TCF7L2

Fig. 3

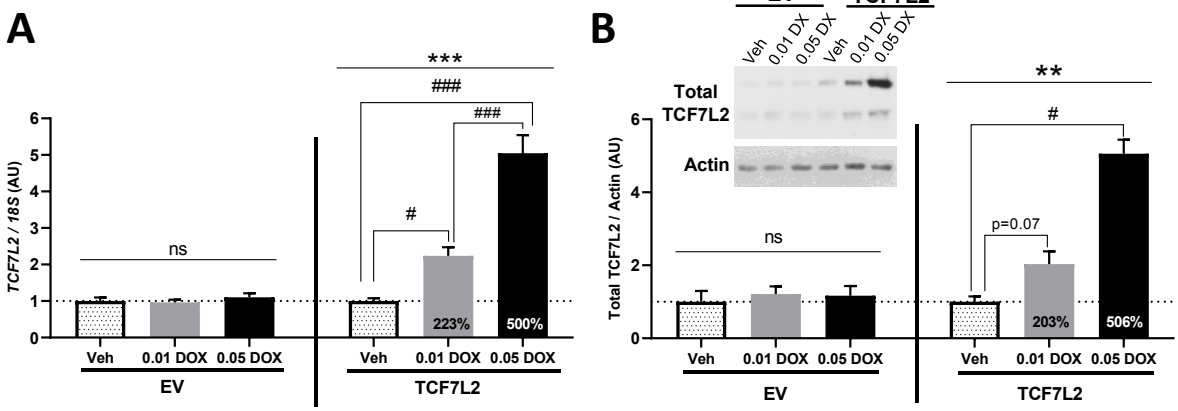
A
TCF7L2 / 18S (AU)
ns
***
###
#
223%
500%
Veh
0.01 DOX
0.05 DOX
EV
TCF7L2

B
EV
TCF7L2
Veh
0.01 DX
0.05 DX
Total TCF7L2
Actin
Total TCF7L2 / Actin (AU)
ns
**
#
p=0.07
203%
506%
Veh
0.01 DOX
0.05 DOX
EV
TCF7L2

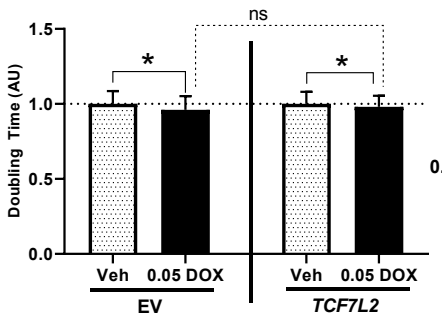
C
Doubling Time (AU)
ns
*
*
Veh
0.05 DOX
EV
TCF7L2

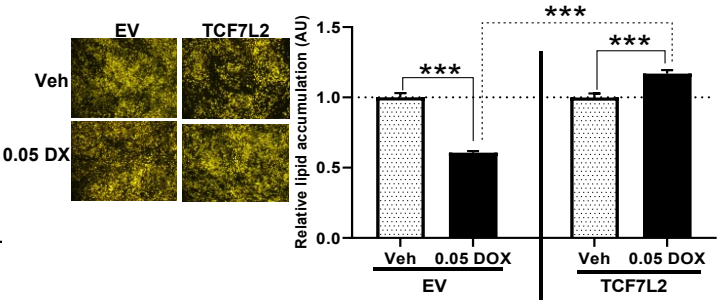
D
EV
TCF7L2
Veh
0.05 DX
Relative lipid accumulation (AU)
***
***
***
Veh
0.05 DOX
EV
TCF7L2

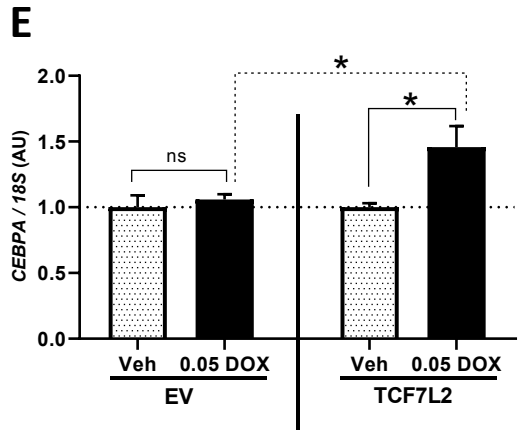
E
CEBPA / 18S (AU)
ns
*
*
Veh
0.05 DOX
EV
TCF7L2

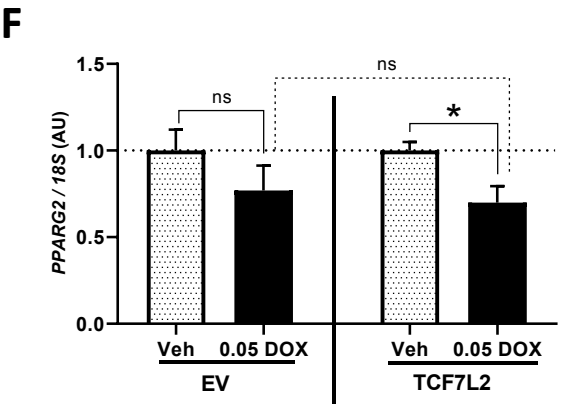
F
PPARG2 / 18S (AU)
ns
ns
*
Veh
0.05 DOX
EV
TCF7L2

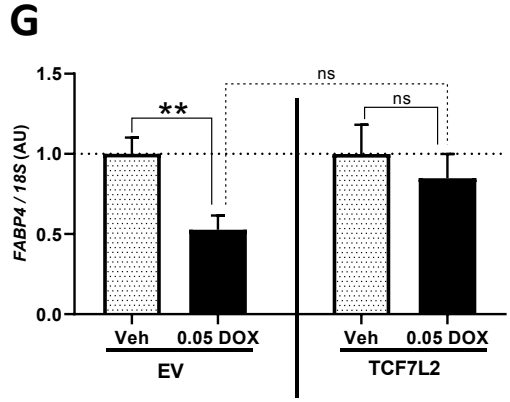
G
FABP4 / 18S (AU)
ns
**
ns
Veh
0.05 DOX
EV
TCF7L2

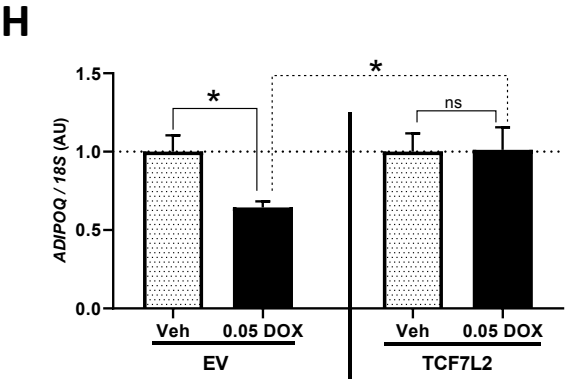
H
ADIPOQ / 18S (AU)
*
*
ns
Veh
0.05 DOX
EV
TCF7L2

Fig. 4

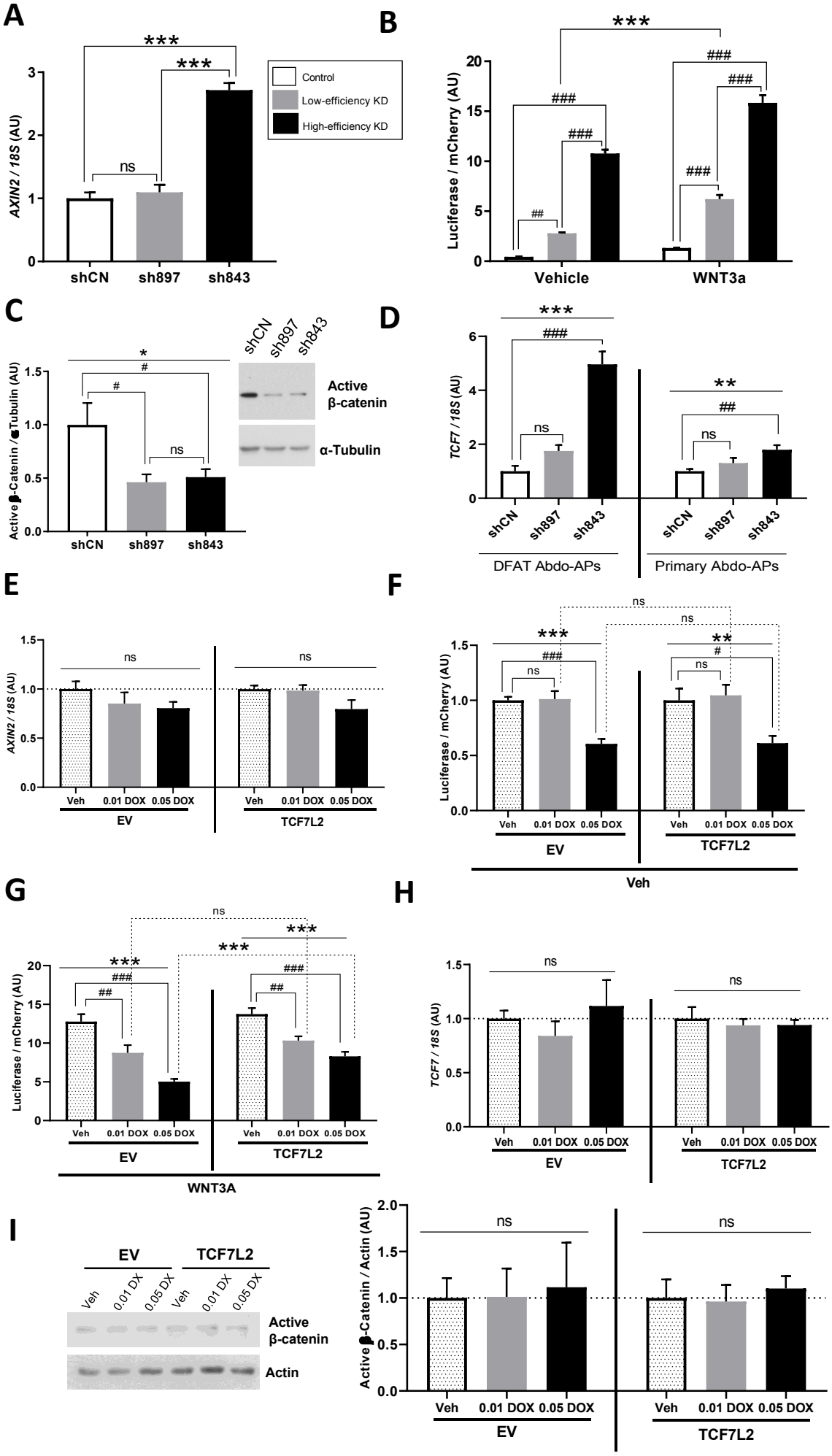
A
B
C
D
E
F
G
H
I
Control
Low-efficiency KD
High-efficiency KD
AXIN2 / 18S (AU)
shCN
sh897
sh843
Luciferase / mCherry (AU)
Vehicle
WNT3a
Active β-catenin / αTubulin (AU)
Active β-catenin
α-Tubulin
TCF7 / 18S (AU)
DFAT Abdo-APs
Primary Abdo-APs
Veh
0.01 DOX
0.05 DOX
EV
TCF7L2
WNT3A
Active β-Catenin / Actin (AU)
Actin
ns

Fig. 5

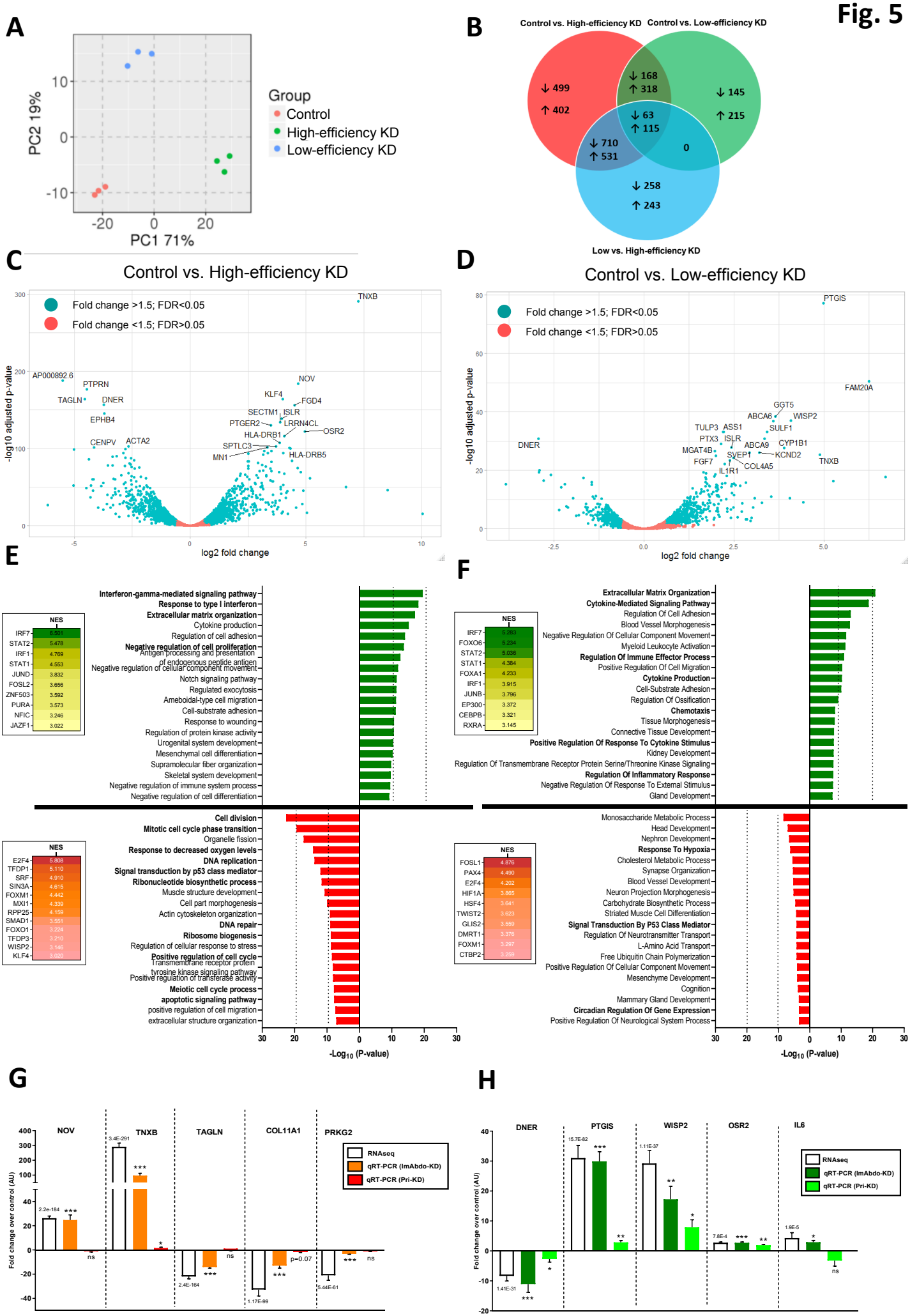
A
PC2 19%
PC1 71%
Group
Control
High-efficiency KD
Low-efficiency KD
B
Control vs. High-efficiency KD
Control vs. Low-efficiency KD
Low vs. High-efficiency KD
↓ 499
↑ 402
↓ 168
↑ 318
↓ 145
↑ 215
↓ 63
↑ 115
↓ 710
↑ 531
0
↓ 258
↑ 243
C
Control vs. High-efficiency KD
Fold change >1.5; FDR<0.05
Fold change <1.5; FDR>0.05
-log10 adjusted p-value
log2 fold change
D
Control vs. Low-efficiency KD
E
F
NES
-Log10 (P-value)
G
NOV
TNXB
TAGLN
COL11A1
PRKG2
RNAseq
qRT-PCR (lmAbdo-KD)
qRT-PCR (Pri-KD)
Fold change over control (AU)
H
DNER
PTGIS
WISP2
OSR2
IL6

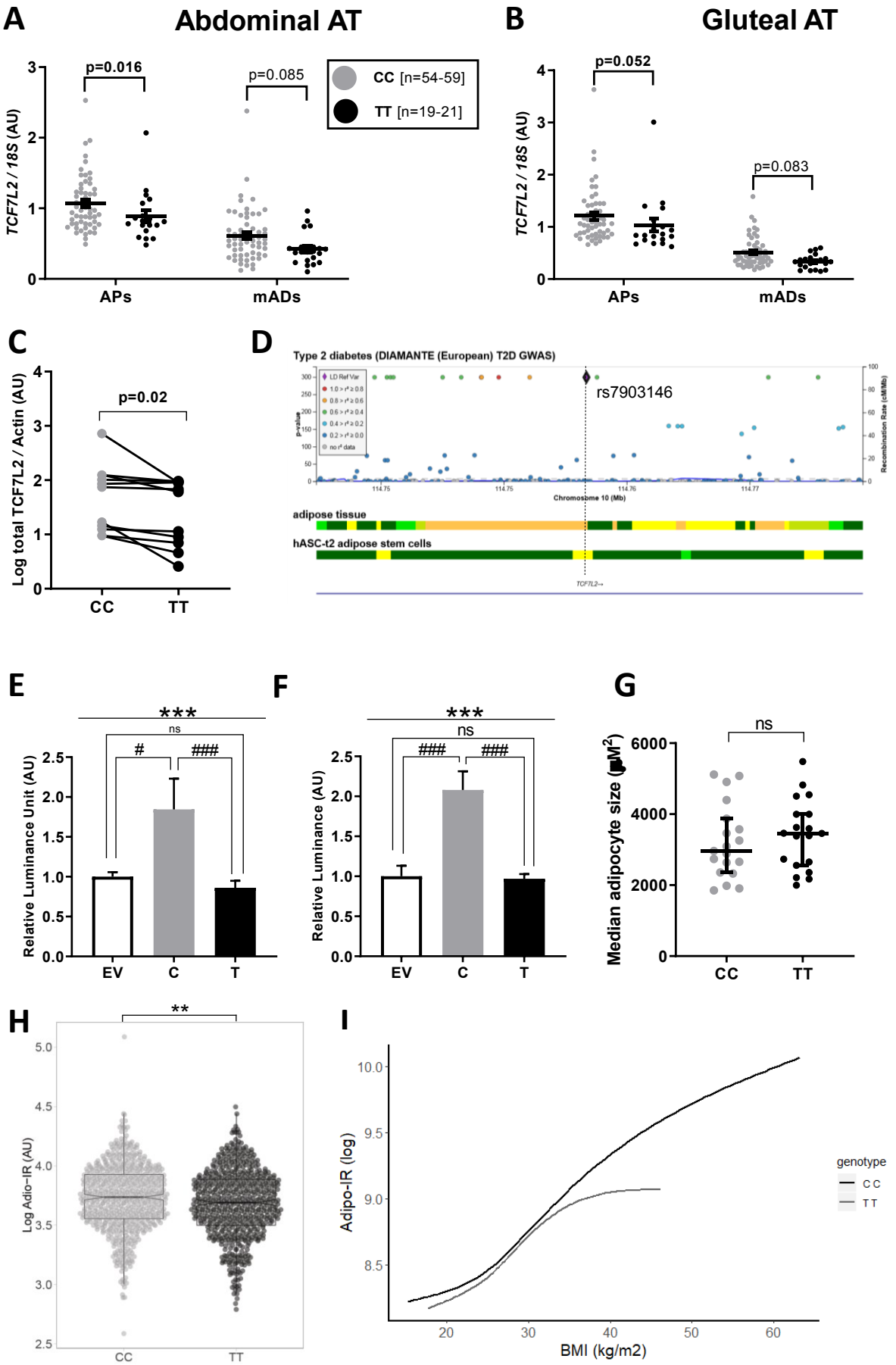
A
Abdominal AT
p=0.016
p=0.085
CC [n=54-59]
TT [n=19-21]
TCF7L2 / 18S (AU)
APs
mADs
B
Gluteal AT
p=0.052
p=0.083
C
p=0.02
Log total TCF7L2 / Actin (AU)
CC
TT
D
Type 2 diabetes (DIAMANTE (European) T2D GWAS)
rs7903146
Chromosome 10 (Mb)
adipose tissue
hASC-t2 adipose stem cells
E
***
ns
#
###
Relative Luminance Unit (AU)
EV
C
T
F
***
ns
###
###
Relative Luminance (AU)
G
ns
Median adipocyte size (µM2)
H
**
Log Adio-IR (AU)
I
Adipo-IR (log)
BMI (kg/m2)
genotype
CC
TT